JOURNAL OF MATERIALS SCIENCE 21 (1986) 1015–1019

Fe–Cr–C hardfacing alloys for high-temperature applications

L.-E. SVENSSON, B. GRETOFT, B. ULANDER, H. K. D. H. BHADESHIA*
*ESAB AB, Gothenburg, Sweden and *Department of Metallurgy and Materials Science, University of Cambridge, Cambridge, UK*

The microstructure and phase chemistry of a Fe–34Cr–4.5C wt% hardfacing alloy has been investigated using transmission electron microscopy and microanalytical techniques. The microstructure is found to consist of large primary M_7C_3 carbides in a eutectic mixture of austenite and more M_7C_3. The results indicate that the microstructure of the undiluted alloy becomes configurationally frozen at a temperature of about 1150° C during deposition by the manual metal arc welding technique. This allows the metastable austenite phase to contain a large chromium concentration (~16 to 17 wt%), thus imparting good corrosion and oxidation resistance. Experimental data on the partitioning of chromium, manganese and silicon between the carbide phases are discussed in the context of the high-temperature stability of the alloy.

1. Introduction

Many common hardfacing alloys are based on iron, sometimes containing large additions of chromium and carbon. The present study is concerned specifically with the characterization of a Fe–34Cr–4.5C wt % alloy deposited by a manual metal arc welding technique. In this condition, the alloy contains a large volume fraction of hard, primary and eutectic chromium-rich carbides in a soft matrix. The carbides, which have a Vickers hardness of 1200 to 1600 HV, provide resistance to wear by coarse sand and hard minerals and the austenite matrix seems to serve as a tough binder. The alloys are generally used at ambient temperature, but the high overall chromium content of the alloy should impart good corrosion and oxidation resistance to temperatures as high as 1000° C. Wear resistance should be maintained at high temperatures because, unlike tungsten carbide which readily decarburizes at temperatures greater than 500° C, the chromium carbide remains stable to beyond 1000° C. The bulk hardness of the alloy is about 700 HV.

The main aim of this study was to investigate whether the matrix phase (austenite, γ) contains enough chromium for adequate high-temperature corrosion and oxidation resistance, since much of the chromium in the alloy should be tied up in the form of carbides. For ambient temperature service in oxidizing conditions, 12 wt % Cr is sufficient to form a continuous, adherent and self-regenerating Cr_2O_3 oxide film which isolates the base metal from the environment. However, to provide adequate corrosion and oxidation resistance at temperatures near 1000° C, a higher chromium concentration of about 17 wt % is found to be necessary [1]. Because of the fine-scale of the matrix phase in the microstructure, the investigation was carried out using microanalytical techniques associated with the transmission electron microscope

2. Experimental details

Hardfacing alloys are usually deposited in three layers to avoid dilution of the top layer by the base material; thicker deposits can lead to extensive weld cracking. The welds were deposited using a manual metal arc welding technique with 4 mm diameter electrodes; the welding conditions are 160 A, 23 V a.c. with a deposition rate of about 0.004 m sec^{-1} (giving a nominal heat input of 920 J mm^{-1}), the interpass temperature being 350° C. The bulk chemical composition of the final (top) layer was found to be Fe–4.46C–33.6Cr–1.19 Mn–0.78Si–0.022S–0.028P (wt %).

Thin foil specimens for transmission electron microscopy were prepared from 0.25 mm thick discs spark machined from the weld deposits. The discs were subsequently thinned and electropolished in a twin-jet polishing unit using a 5% perchloric acid, 25% glycerol and 70% ethanol mixture at ambient temperature and 55 V. The foils were examined in a Philips EM400T transmission electron microscope operated at 120 kV. Microanalysis experiments were also carried out on this microscope, using an energy-dispersive X-ray analysis facility. The specimens, which were about 100 nm thick in the areas of interest, were held in a beryllium holder tilted 35° from the normal which is equal to the take off angle. The X-ray count rate was optimized to about 200 counts sec^{-1} over a count period of 100 sec giving a typical statistical accuracy of ±1%. The data were analysed using the LINK RTS 2 FLS program for thin foil microanalysis; this corrects the data for atomic number and absorption and accounts for overlapping peaks by fitting standard profiles. Even though the probe diameter used was about 3 nm, beam spreading due to scattering of electrons within the thin foil gave an estimated broadened beam diameter of 20 nm. This did not cause any difficulties since the scale of the microstructure is comparatively large. The elements analysed were iron, silicon, manganese and chromium;

0022–2461/86 $03.00 + .12

none of these cause significant fluorescence effects in thin foil samples. The absence of fluorescence or surface contamination layer effects was verified since microanalysis of regions of differing thickness within the same carbide particle gave very similar results. Nockolds *et al.* [2] have suggested the presence of significant fluorescence effects in thin foil samples of Fe–Cr alloys, but Twigg and Fraser [3] have pointed out the conflicting results in this area. Our calculations using Bourdillon's [4] method show that for a Fe–51Cr at % alloy, the fluorescence correction is very small and reduces the chromium concentration to 50.2 at % for a foil thickness of 100 nm.

The error bars stated in the present work are those quoted by the Link system and represent a conservative overestimate of the statistical error.

The beryllium window on the detector used in the microanalysis system absorbs X-rays from light elements so that carbon could not be analysed; this means that the microanalytical data have to be corrected for the presence of carbon. In the discussion that follows, y_i refers to the concentration of element "i" in weight percent, when the presence of carbon is ignored. The true concentration (wt %) is denoted x_i; z_i refers to the ratio of the number of atoms of i to the total number of substitutional atoms.

It follows that for substitutional atoms,

$$y_i = 100w_i/(w_{Fe} + w_{Si} + w_{Mn} + w_{Cr}) \quad (1a)$$

where w_i is the weight of element i.

$$z_i = (y_i/A_i)/[(y_{Fe}/A_{Fe}) + (y_{Si}/A_{Si}) + (y_{Mn}/A_{Mn}) + (y_{Cr}/A_{Cr})] \quad (1b)$$

where A_i is the atomic weight of element i. The true concentration in wt % is given by

$$x_i = 100w_i/(w_{Fe} + w_{Si} + w_{Mn} + w_{Cr} + w_C) \quad (1c)$$

For a stoichiometric M_7C_3 carbide,

$$x_C = 300A_C/M \quad (1d)$$

where $M = 7(z_{Fe}A_{Fe} + z_{Cr}A_{Cr} + z_{Mn}A_{Mn} + z_{Si}A_{Si}) + 3A_C$ and for the substitutional alloying elements we have

$$x_i = 700z_iA_i/M \quad (1e)$$

Similarly, if the carbon content of the austenite is known, then the corresponding x_i for γ can be calculated.

Most of the microanalysis work was carried out using transmission electron microscopy, but it proved difficult to obtain thin foil specimens containing the large primary carbides and their surrounding regions. These areas were therefore analysed in a scanning electron microscope fitted with a Link energy dispersive X-ray analysis system; the Link microanalysis program in this case corrected for fluorescence as well as atomic number and absorption effects.

3. Results and discussion

If the small amounts of manganese and silicon are ignored, then the liquidus projection of the Fe–Cr–C system (Fig. 1a) indicates that primary M_7C_3 carbide is the first phase to form on cooling below the liquidus

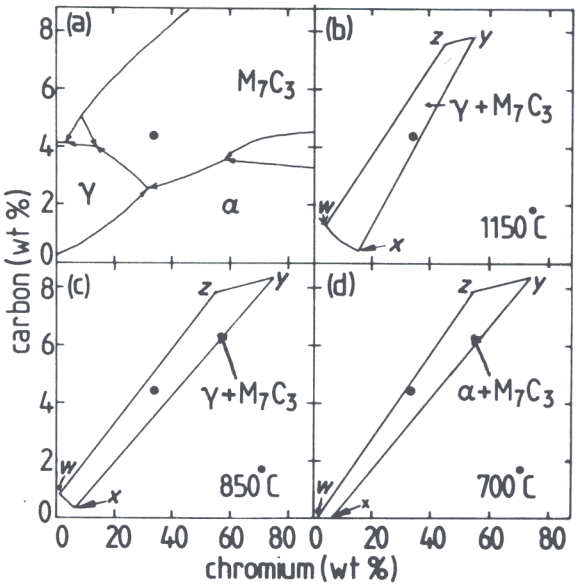

Figure 1 (a) Liquidus projection of the Fe–Cr–C system [5]; (b to d) the $\gamma + M_7C_3$ or $\alpha + M_7C_3$ phase fields (*wxyz*) in isothermal sections of the Fe–Cr–C system [5]. The approximate composition (i.e. ignoring manganese and silicon) of the alloy used is indicated (●) in each figure.

temperature; the residual liquid should then decompose via a eutectic reaction into austenite and more M_7C_3 eutectic carbides. Consistent with this, optical microscopy shows the presence of large primary carbides which have a faceted morphology (Fig. 2). These primary carbides are assumed to be M_7C_3 carbides, consistent with the microanalytical results given in Table I. They are surrounded by precipitate free zones, probably due to chromium depletion of the liquid in their vicinity – the γ near the primary carbides has a chromium level comparable to that of the eutectic austenite (Table I), implying that it is not

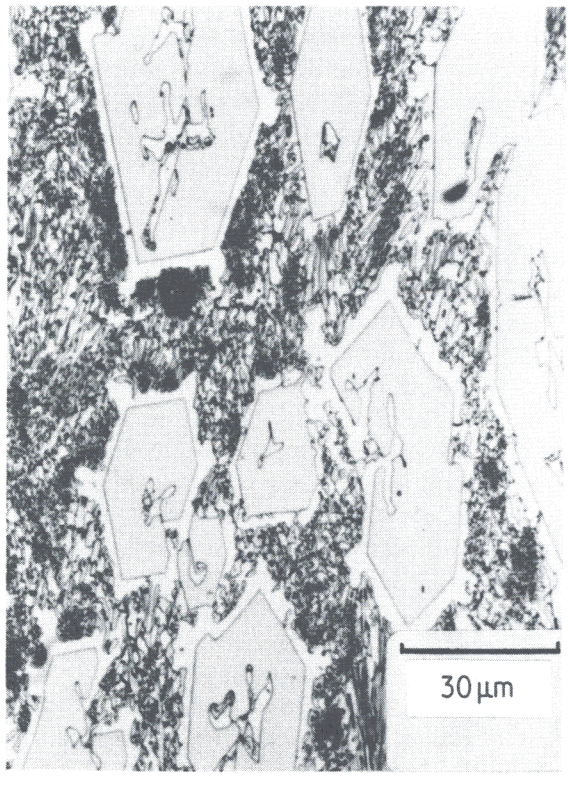

Figure 2 Optical micrograph of the top layer.

TABLE I Mean compositions of eutectic phases (error estimates can be obtained from Fig. 4). The results are quoted to two decimal places for internal consistency. The carbon concentrations are deduced as discussed in the text. The results for the primary carbides and the austensite around the primary carbides are obtained using scanning electron microscopy, and represent the mean of two tests in each case (the errors are comparable to those illustrated in Fig. 4)

	Eutectic γ		Eutectic M_7C_3		Primary M_7C_3		γ near primary M_7C_3	
	y_i	x_i	y_i	x_i	y_i	x_i	y_i	x_i
Fe	80.64	80.29	37.21	33.94	42.40	38.68	77.76	77.41
Si	1.70	1.69	0.18	0.16	0.18	0.16	1.86	1.85
Mn	1.15	1.14	1.56	1.43	0.99	0.90	1.39	1.38
Cr	16.51	16.43	61.05	55.67	56.43	51.47	18.99	18.91
C		0.45		8.80		8.78		0.45

supersaturated with respect to the carbide phase. The remaining microstructure consists of a eutectic mixture of finer M_7C_3 carbides in an austenitic matrix, as confirmed by transmission electron microscopy and electron diffraction (Fig. 3).

The austenite was found to contain a large number of stacking faults (Fig. 3) and this is probably because chromium lowers the stacking fault energy of austenite [6]. M_7C_3 has a complex hexagonal lattice ($D10_1$ structure, with $a = 1.398$ nm and $c = 0.451$ nm for M_7C_3 of present composition [7]) and the resulting small c/a ratio means that the basal plane is not close-packed. Faulting therefore usually occurs on the prism planes; the eutectic M_7C_3 always appears streaked (Fig. 3) and this is believed to be due to such faulting.

The results from microanalysis experiments on the eutectic structure are presented in Fig. 4 and the mean concentrations are summarized in Table I. The carbon

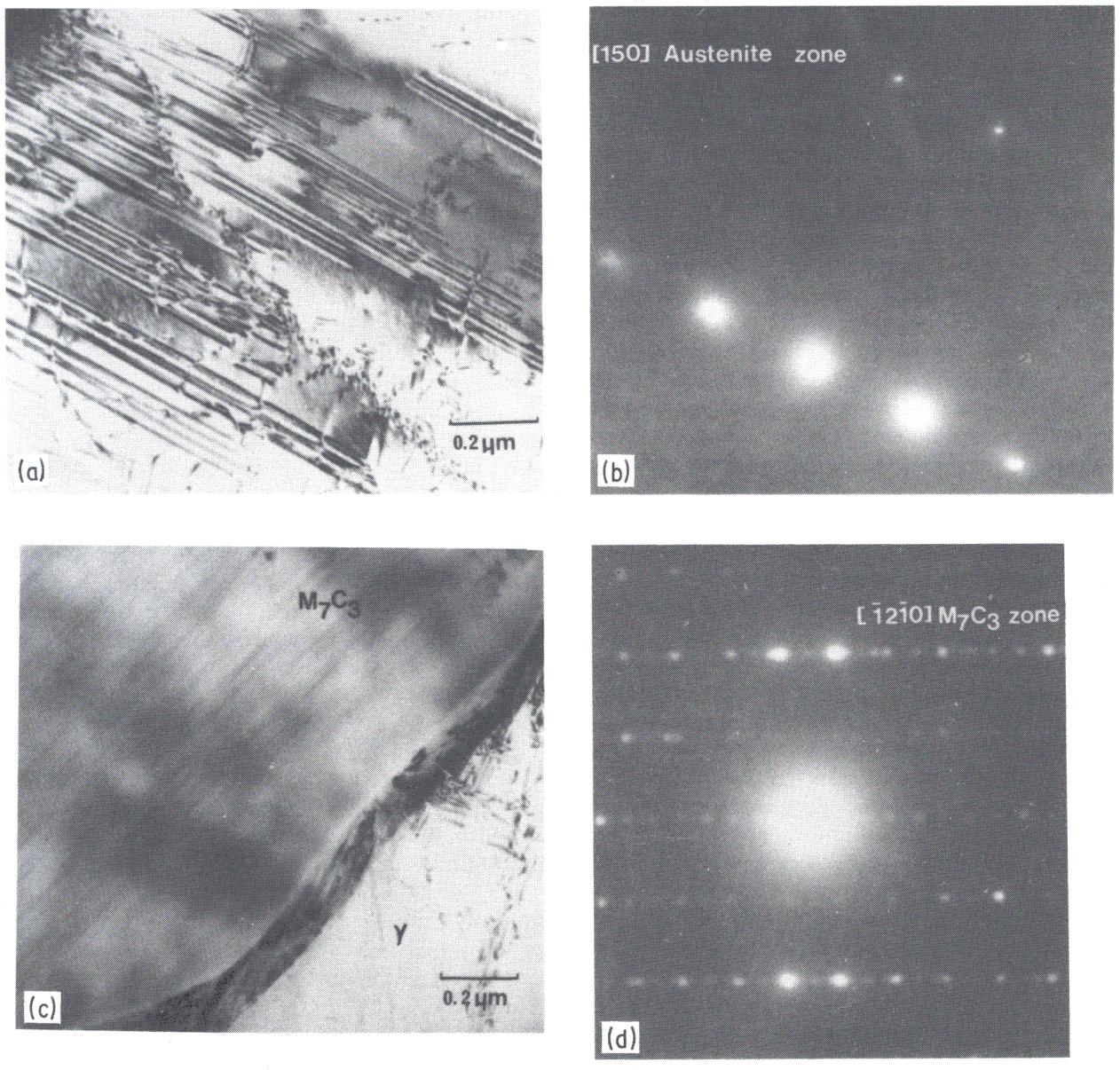

Figure 3 (a and b) Transmission electron micrograph and corresponding electron diffraction pattern from the austenite matrix; (c and d) transmission electron micrograph and corresponding electron diffraction pattern from eutectic M_7C_3.

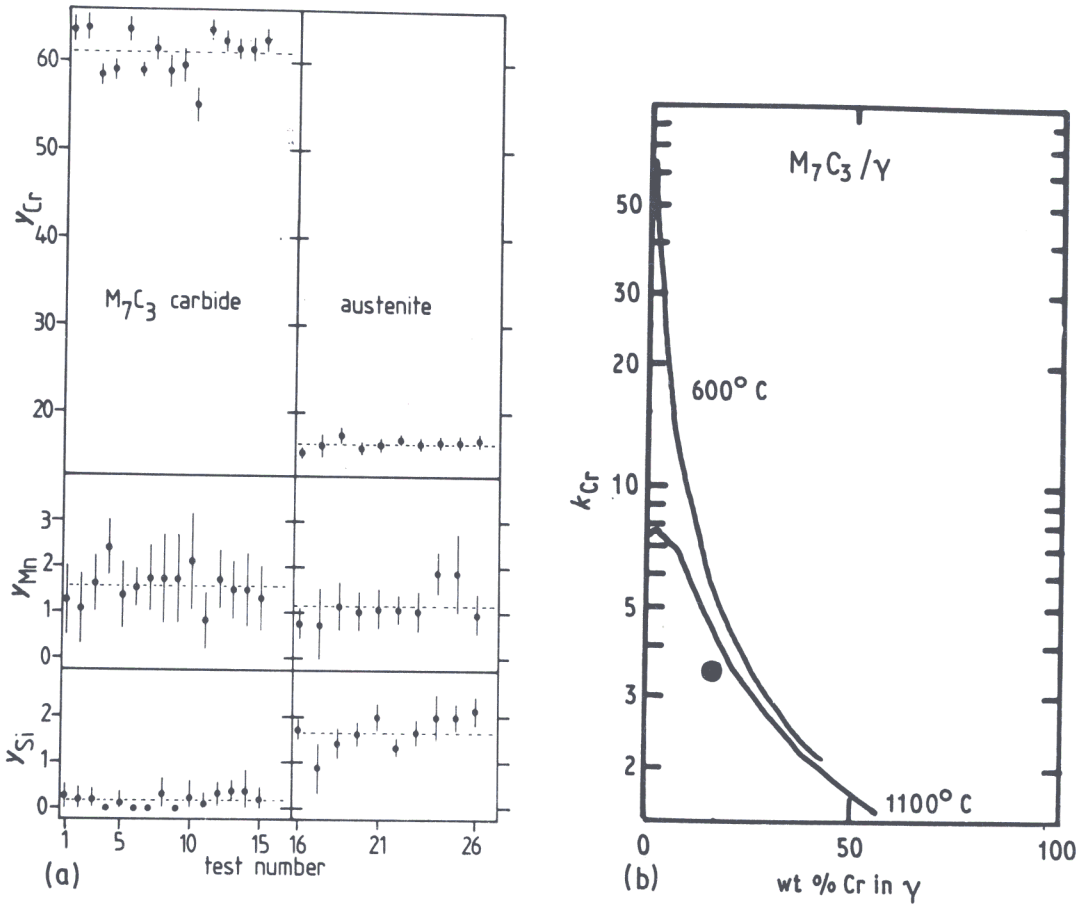

Figure 4 (a) Microanalytical (TEM) data on eutectic M_7C_3 and γ phases (y_i has units of wt % and is defined in Equation 1a). Note that the tests are done at random positions; (b) partitioning coefficients for the Fe–Cr–C system [8]. The partitioning coefficient for the experimental alloy (●) indicates that the as-deposited microstructure is frozen from about 1150° C.

content of the carbide is deduced assuming stoichiometry and that of the austenite is estimated from the Fe–Cr–C phase diagram, as discussed later.

Focusing now on the eutectic regions, neither the γ nor the M_7C_3 showed significant composition variations between the different regions analysed. This is probably because both the M_7C_3 and γ (of the eutectic) can co-exist over a narrow composition range; in Figs. 1b to d, the lines zy and wx represent the possible M_7C_3 and austenite (or ferrite) compositions, respectively. The iron content of the M_7C_3 carbide was in all cases found to be consistent with the fact that M_7C_3 is known [5] to dissolve up to 55 wt % of iron, and the carbide clearly rejects silicon (Fig. 4) while manganese preferentially partitions into the carbide phase. The austenite on average contains 16.4 wt % chromium (slightly lower than the γ near the primary carbide) and this is just adequate to provide corrosion and oxidation resistance at high temperatures.

In the discussion that follows, the presence of small amounts of manganese and silicon in the alloy are ignored, the microstructure being discussed in terms of the Fe–Cr–C phase diagram. In each of Figs. 1b to d, the point x defines the maximum chromium content possible in the eutectic γ or α (henceforth referred to as x^m_{Cr}), when either of these phases is in equilibrium with M_7C_3. x^m_{Cr} clearly decreases with decreasing temperature. The microanalysis results (Fig. 4, Table I) and the fact that the matrix phase is γ (rather than α) strongly suggests that the as-deposited microstructure is far from equilibrium. The equilibrium microstructure of the alloy is in fact $\alpha + M_7C_3$, as illustrated in Fig. 1d. Even at 1150° C, $x^m_{Cr} = 15.1$ wt %, whereas it is experimentally found that the γ contains about 16.4 wt % Cr. The observed microstructure is therefore configurationally frozen at some temperature just above 1150° C, and it is this structure which is retained to ambient temperature without further change. All this is a consequence of the high cooling rates (typically 20 to 30° C sec^{-1} over the temperature range 800 to 500° C) involved in manual metal arc welding and the fact that all of the transformations necessary to accomplish equilibrium require thermally activated, long-range diffusion. The experimentally determined partition coefficient $k_{Cr} = 3.4$ (ratio of x_{Cr} in M_7C_3 to that in γ, Fig. 4) is also consistent with reactions stopping at $T > 1100°$ C (Fig. 4). The melting point of the alloy is about 1380° C, so that the entire microstructure can be considered to have formed within the narrow temperature range 1380 to 1150° C.

The phase diagram indicates that service at temperatures between 850 to 1150° C must lead to a gradual equilibration of the system, with a decrease in the γ chromium content. Extended service at lower temperatures (e.g. 700° C) must cause the γ to diffusionally transform to α with a further decrease in matrix chromium concentration. These changes are thermodynamically favoured, but the time scale over which they occur is a function of kinetics, and initial

experiments suggest that the changes might be very sluggish, since they involve long-range substitutional atom diffusion. The alloy only seems to undergo significant oxidation at temperatures around 1050° C [9], probably because the carbide phase, which occupies a major part of the microstructure, contains some 55 wt % Cr.

4. Conclusions

The chromium concentration of the austenite matrix of Fe–34Cr–4.5C wt % hardfacing alloy is sufficiently high to provide oxidation and corrosion resistance at high temperatures. The microstructure of the alloy, as deposited by a manual metal arc welding technique, is that retained from a temperature just above 1150° C. The as-deposited $M_7C_3 + \gamma$ microstructure is thus metastable, and given sufficient thermal activation, should tend to equilibrate. Equilibration could involve a reduction in the chromium content of the γ ($T > 700°$ C), or the decomposition of γ into α (with lower chromium content) and M_7C_3 at temperatures around 700° C. The kinetics of the equilibration processes are not known and require further investigation. The work indicates that the alloy has good potential for high temperature applications.

Acknowledgments

The authors are grateful to ESAB AB (Sweden) for financial support and for the provision of laboratory facilities, and to Professor D. Hull for the provision of laboratory facilities at the University of Cambridge. Helpful discussions with Dr A. J. Bourdillon on aspects of microanalysis are gratefully acknowledged.

References

1. J. C. SCULLY, "The Fundamentals of Corrosion", 2nd Edn. (Pergamon Press, Oxford, 1981) p. 45.
2. C. NICKOLDS, M. J. NASIR, G. CLIFF and G. W. LORIMER, Institute of Physics Conference Series No. 52 (Institute of Physics, 1980) Ch. 9, p. 417.
3. M. E. TWIGG and H. L. FRASER, in "Microbeam Analysis", edited by K. F. J. Heinrich (San Francisco Press, California, 1982) p. 37.
4. A. J. BOURDILLON, Proceedings of the 40th EMSA meeting, Washington, edited by G. W. Bailey (Claitors Publishing Division, Baton Rouge, 1982) p. 510.
5. "Metals Handbook", Vol. 8 (American Society for Metals, Ohio, 1973) p. 402.
6. R. E. SCHRAMM and R. P. REED, *Metall. Trans.* **6A** (1975) 1345.
7. D. J. DYSON and K. W. ANDREWS, *J. Iron Steel Inst.* **207** (1969) 209.
8. B. UHRENIUS, in "Hardenability Concepts with Applications to Steel", edited by D. V. Doane and J. S. Kirkaldy (Metals Society AIME, USA, 1977) p. 28.
9. L. E. SVENSSON, unpublished research ESAB AB, Sweden (1985).

Received 20 February
and accepted 30 May 1985